

Pattern of breast cancer blood flow and metabolism, assessed using dual-acquisition ^{18}FDG PET : correlation with tumor phenotypic features and pathological response to neoadjuvant chemotherapy

Olivier Humbert^{1,2}; Maud Lasserre² ; Aurélie Bertaut³ ; Pierre Fumoleau⁴ ; Charles Coutant⁵ ; François Brunotte^{2,6,7} ; Alexandre Cochet^{2,6,7}

¹ Department of Nuclear Medicine, Centre Antoine-Lacassagne, Université Côte d'Azur, Nice, France

² Department of Nuclear Medicine, Centre GF Leclerc, Dijon, France;

³ Department of Biostatistics, Centre GF Leclerc, Dijon, France;

⁴ Department of Medical Oncology, Centre GF Leclerc, Dijon, France;

⁵ Department of Surgery, Centre GF Leclerc, Dijon, France;

⁶ Imaging Department, CHU Le Bocage, Dijon, France ;

⁷ Le2i FRE2005, CNRS, Arts et Métiers, Univ. Bourgogne Franche-Comté

Corresponding author:

Olivier Humbert

Centre Antoine Lacassagne, 33 Avenue de Valombrose, 06100 NICE

Telephone: +33-4-92031148

Fax: +33-4-92031572

Email: ohumbert@unice.fr

Word count (without supplemental figures and tables) = 4999

The authors have no disclosure or financial support to declare.

Running title: FDG PET in breast cancer

ABSTRACT

In breast cancer, early changes in tumor glucose metabolism and blood flow (BF) have been evaluated separately and are proposed to monitor tumor response to neoadjuvant chemotherapy (NAC). This study used a single ¹⁸FDG dual-acquisitions PET exam to simultaneously assess these imaging features and to answer two questions: (i) Do tumor blood flow (BF) and tumor metabolism correlated with the same pre-therapy tumor phenotypic features? (ii) Are early changes in tumor BF and metabolism in response to NAC comparable or complementary in the ability to predict the pathological complete response (pCR)?

Methods: 150 women with breast cancer and an indication for NAC were prospectively included. Women had a baseline PET exam with a 2-min chest-centered dynamic acquisition, started at the time of ¹⁸F-FDG injection, followed by a delayed static PET acquisition performed at 90 min. Tumor BF was calculated from the dynamic image using a validated first-pass model, and tumor glucose metabolism (SUV_{max}) was calculated on the delayed acquisition. This dual-PET acquisition was repeated after the first cycle of NAC to measure early changes in tumor BF (ΔBF) and SUV_{max} (ΔSUV_{max}).

Results: A weak correlation was found between baseline tumor SUV_{max} and BF ($r= 0.22$; $p=0.006$). A higher baseline SUV_{max} was associated with all biological markers of tumor aggressiveness, including the Triple Negative Breast Cancer (TNBC) subtype ($p<0.0001$). In contrast, a high baseline tumor BF was only associated with obesity ($P=0.002$). Mean ΔSUV_{max} was $-44.6\pm27.4\%$ and varied depending on the SBR grade, the overexpression of HER2+ and the lack of hormonal receptor expression ($p=0.04$, $p<0.001$ and $p=0.01$, respectively). Mean ΔBF was $-26.9\pm54.3\%$ and a drastic reduction was only observed in HER2-positive subtypes ($-58.7\pm30.0\%$), supporting the

anti-angiogenic effect of Trastuzumab. Changes in tumor glucose metabolism outperformed changes in BF to predict pCR in all tumor subtypes: The Areas Under the Curve of ΔSUV_{\max} were 0.82, 0.65 and 0.90 in the TNBC, HER2-positive and Luminal subtypes, respectively.

Conclusion: Of the two biological hallmarks of cancer evaluated in this study, the reduction in tumor metabolism was more accurate than the reduction in BF to predict pCR in the different subtypes of breast cancer.

Keys words: FDG PET, blood flow, metabolism, breast cancer, response.

INTRODUCTION

Neoadjuvant chemotherapy (NAC) for breast cancer is as a therapeutic approach for women with a large primary tumor. The clinical benefit of NAC is that it increases the rate of breast-conservative surgery (1). NAC, as compared with conventional adjuvant chemotherapy, does not improve patients' outcomes (1). Nonetheless, studies have demonstrated that a pathological complete response (pCR) at the end of NAC is an important surrogate marker of a favorable outcome (2,3). Thus, pCR has become a crucial end-point in the neoadjuvant setting.

Angiogenesis and cell energy deregulation are two hallmarks of oncogenesis (4). In the neoadjuvant setting of breast cancer, both tumor characteristics have been evaluated through different imaging modalities to assess the tumor response to treatment. Early changes in tumor metabolism have been mainly assessed with ¹⁸Fluoro-deoxy-glucose Positron Emission Tomography (¹⁸FDG-PET), while changes in tumor blood flow have been assessed using various modalities, including dynamic contrast enhanced-magnetic resonance imaging (DCE-MRI) and ¹⁵O-water PET.

Using ¹⁸FDG-PET, tumor glucose metabolism is usually quantified using the Standardized Uptake Value (SUV) (5–7). In the neoadjuvant setting of breast cancer, treatment-related changes in tumor metabolism (Δ SUV) has been reported to be a strong predictor of the pathological response after the first or second cycle of NAC (5–9).

Different imaging modalities, such as DCE-MRI, ¹⁵O-water PET and 1-hour-dynamic ¹⁸FDG PET imaging (FDG-K1), can yield kinetic parameters reflecting vascular permeability and perfusion. The quantification of tumor blood flow with these modalities has been reported to

provide predictive and prognostic information while monitoring the effects of NAC (10–15). Because an on-site cyclotron is needed for ¹⁵O-water PET studies and because a one-hour full-dynamic ¹⁸FDG-PET acquisition is hardly suitable in routine practice, there was a need to develop new analysis methods. To this end, Mullani et al developed a 2-min dynamic first-pass PET acquisition based on a one-compartment flow model to assess tumor blood flow (16,17).

The relationship and incremental value between the tumor metabolic and blood flow response to NAC in breast cancer has not yet been fully elucidated. By using a single ¹⁸FDG- dual-acquisition PET exam to assess tumor metabolism and blood flow, this study aimed to answer two important questions: (i) Do tumor blood flow (BF) and tumor metabolism correlated with the same pre-therapy tumor phenotypic features? (ii) Are early changes in blood flow comparable or complementary to early changes in glucose metabolism in their ability to predict the final pathological response in patients with breast cancer?

MATERIALS AND METHODS

Patients and Study Design

From February 2009 to October 2014, women referred to the Centre G.F. Leclerc for clinical stage II or III biopsy-proven breast cancer with an indication for neoadjuvant chemotherapy were prospectively evaluated. This population overlaps those of previous articles published by our team (8,9,17–20). Patients with high glycemia (>9 mmol/l), those unwilling to undergo the complete PET exams and those with metastasis on the baseline ¹⁸F-FDG PET were excluded. The institutional review board approved this prospective study as a current care study. The medical

team documented the non-opposition of the patient in source documents and on the information notice provided to the patient, the signature of written informed consent was waived.

Tumor size and lymph node involvement were evaluated on ultrasound (US) scan. The women underwent different neoadjuvant chemotherapy regimens. Briefly, all women with Human Epidermal Growth Factor Receptor-2 (HER2)-positive tumors were treated with trastuzumab and docetaxel-based regimens. Women with triple negative or luminal/HER2-tumors received 6 cycles of sequential chemotherapy with anthracyclines and taxanes, or six cycles of FEC100.

Within one month after the last course of chemotherapy, the tumors were surgically removed. A pCR was defined as no residual invasive cancer in the breast and nodes, though in-situ breast residuals were allowed (ypT0/is ypN0) (3).

¹⁸F-FDG-PET Procedures

A first ¹⁸F-FDG-PET scan was done at baseline (Gemini GXL PET/Computed Tomography (CT) and Gemini TF PET/CT scanners). Patients were instructed to fast for at least 6 hours before the intravenous injection of 5 MBq/kg of ¹⁸F-FDG for Gemini GXL studies and 3 MBq/kg for Gemini TF studies.

¹⁸F-FDG was injected using an automatic PET infusion system (Intego; Medrad) at a rate of 1 mL/s. Simultaneously with the injection, the first chest-centered emission acquisition with the patient in the prone position, using a breast imaging coil, was run in the list mode for 2 minutes, followed by a low-dose CT scan. Reconstructions of 5 and 10-second frames were extracted. Sixty minutes after the ¹⁸F-FDG injection, a whole-body PET scan was done. Finally, 90 min after the

injection, a PET scan restricted to the chest (2 bed positions) with patients in the prone position, was performed.

A few days before the second course of chemotherapy, a second ^{18}F -FDG PET scan was performed with the same chest-restricted early dynamic first-pass and late PET static acquisitions at 90 min.

First-pass Model to Measure Tumor Blood Flow. The concept and method for measuring tumor blood flow from the first pass of ^{18}F -FDG has been explained in a previous paper from our institution (17). It is based on the first-pass model of Mullani et al. described in previous reports (16,21). Volumes of interest (VOI) encompassing the primary tumor and the ascending aorta were manually delineated using the 2-min dynamic summed functional and anatomical images. Tumor BF at baseline (BF1) and after the 1st cycle of chemotherapy (BF2) were then calculated in $\text{mL} \cdot \text{min}^{-1} \cdot \text{g}^{-1}$ of tumor using the following equation (16) :

$$BF = \frac{Q(T_m)}{E \times \int_0^{T_m} Ca(t)dt \times V_t}$$

$Q(T_m)$ is the amount of the tracer in tumor tissue at time T_m measured with the tumor VOI, E is the tumor first-pass extraction fraction of ^{18}F -FDG which is assumed to be equal to 1 (15), $Ca(t)$ is the arterial concentration of the tracer at time t measured with the aorta VOI. V_t is the tumor volume (mL) delineated using the 2-min dynamic summed functional and anatomical images.

The tumor blood flow response to chemotherapy was calculated:

$$\Delta BF (\%) = 100 \times (BF2 - BF1) / BF1$$

Tumor Glucose Metabolism Measurements. A spheroidal VOI encompassing the primary tumor was drawn on the 90 min chest-restricted acquisitions to measure the baseline SUV_{\max} ($SUV1_{\max}$),

corrected for body weight, and after the first course of chemotherapy ($SUV2_{max}$). The metabolic response to treatment was calculated :

$$\Delta SUV_{max} (\%) = 100 \times (SUV2_{max} - SUV1_{max}) / SUV1_{max}.$$

The ratio between baseline tumor glucose metabolism and blood flow ($SUV1_{max}/BF1$) was calculated.

Statistical Analyses

Continuous variables were expressed as medians with ranges, or means with standard deviations (SD) and compared using Student's test or non-parametric tests depending on the normality of the distribution. Correlations between PET variables were determined using Pearson's correlation coefficient (r). Qualitative variables were expressed as percentages and compared using the Chi-2 or Fisher's test.

Receiver operating characteristic curves (ROC) were used to compare the predictive values of the different blood flow and metabolic PET parameters for pCR. The Areas Under the Curve (AUC) were calculated with their 95% Confidence Intervals (95% CI). A logistic regression model was also built to combine two different variables in ROC curves analyses. All analyses were performed using SAS 9.4. software. The significance level was set at 0.05 except for multiple comparisons which were handled using the Bonferroni correction (22).

RESULTS

Patients' Characteristics (Table 1).

One hundred and fifty patients were included. The patients' median age was 49 years (range, 23-85 years). The median primary tumor size, assessed with breast ultrasound and/or

mammogram, was 3.3 cm (range, 1.4-10 cm). The tumor subtype in most patients was luminal/HER2-negative (40.7%), followed by HER2-positive (31.3%) and TNBC (28%). pCR was achieved in 26% of women (39/150). The time from tracer injection to delayed breast acquisition was 84.8 ± 8.3 [68-112] min. on the baseline PET study and 85.6 ± 8.6 [66-110] min. on the interim PET study. The glucose serum level was 5.2 ± 0.7 [2.9-7.6] mmol.L⁻¹ on the baseline PET study and 5.4 ± 0.9 [3.8-9.4] mmol.L⁻¹ on the interim PET study.

Correlation Between Baseline FDG Uptake, BF and Clinical/Histopathological Parameters.

A weak correlation was found between tumor SUV_{1max} and BF1 ($r= 0.22$; $p=0.006$) (Fig.1). Mean tumor SUV_{1max} was 10.2 (SD=5.9) but differed significantly depending on the tumor subtype with the highest value observed in the TNBC subtype ($p<1.10^{-4}$) (Table 2; Supplemental Fig.1). Mean tumor BF1 was 0.21 (SD=0.13) ml.min⁻¹.gr¹ and did not differ according to the different breast cancer subtypes ($p=0.61$) (Table 2).

After multiple comparisons correction ($n=10$, p cut-off = 0.005), a high SUV_{1max} was significantly associated with the biological markers of tumor aggressiveness: a high tumor grade (SBR3, $p<0.001$), negative hormonal receptor status ($p<0.001$) and a high mitotic score ($p<0.001$) (table 3). In contrast, BF1 correlated with the patient's Body Mass Index (BMI) only (cut-off = 30): BF1 was 0.19 (SD=0.12) ml.min⁻¹.g⁻¹ in normal weight women versus 0.26 (SD=0.12) ml.min⁻¹.g⁻¹ in obese women ($p=0.002$).

Response after the 1st cycle of NAC

Mean Δ SUV_{max} and Δ BF were -44.6% (SD=27.4%) and -26.9% (SD=54.3%), respectively. A moderate correlation was observed between Δ SUV_{max} and Δ BF ($r=0.52$, $p<0.001$) (Fig.2). Δ SUV_{max}

varied depending on the SBR grade, the overexpression of HER2+ and the lack of hormonal receptor expression ($p=0.04$, $p<0.001$ and $p=0.01$, respectively). But after multiple comparisons correction, a higher ΔSUV_{\max} and ΔBF were only associated with the overexpression of HER2 ($p<0.001$; Table 2 and 3).

Prediction of pCR, all Tumors Pooled Together (Suppl.Table 1; Fig.3, supplemental Fig.2).

Concerning tumor glucose metabolism, ΔSUV_{\max} was the best parameter to predict pCR. It showed good diagnostic accuracy on ROC analysis ($\text{AUC}=0.82$; 95% CI 0.74-0.89; $p<0.0001$). The pCR rate of patients with ΔSUV_{\max} under or over the median percentage value was 45.3% (34/75) and 6.7% (5/75), respectively ($p<10^{-4}$). Concerning tumor blood flow, ΔBF was the best parameter to predict pCR but showed poor diagnostic accuracy on the ROC analysis ($\text{AUC}=0.65$; 95% CI 0.55-0.74; $P=0.003$). The pCR rate of patients with ΔBF under or over the median percentage value was 32.0% (24/75) and 20.0% (15/75), respectively ($p=0.09$). Combining ΔBF and ΔSUV in ROC analysis, the logistic procedure indicated that the AUC for the combined prediction rule did not improve the predictive value in comparison with ΔSUV alone.

Prediction of pCR with a per-Subtype Analyses (Supplemental Table 1; Fig.3, supplemental Fig.2). In triple-negative tumors, ΔSUV_{\max} outperformed the other PET parameters to predict pCR with an AUC of 0.82 (95% CI = 0.68-0.95; $p<0.0001$). SUV2_{\max} had a lower but still fair accuracy ($\text{AUC}=0.75$; 95% CI = 0.59-0.91; $p=0.003$). ΔBF and BF2 had poorer accuracies ($\text{AUC}=0.66$ and 0.68, respectively, $p=0.05$ and 0.04, respectively). SUV1_{\max} , BF1 and the $\text{SUV1}_{\max}/\text{BF1}$ ratio failed to predict pCR ($\text{AUC}<0.60$). The ROC curve analysis combining ΔBF and ΔSUV did not increase the AUC to predict pCR.

In patients with HER2-positive tumors, a high ΔSUV_{\max} was predictive of pCR, with low

accuracy (AUC=0.66, p=0.05). A low SUV2 had a low and not significant accuracy (AUC=0.65, p=0.09). SUV_{1max}, BF1, BF2, ΔBF and the SUV_{1max}/BF1 ratio failed to predict pCR (AUC<0.60)

Among the 61 patients with luminal/HER2- cancer, only three achieved a pCR at the end of NAC. Despite this small number of pCR, a high SUV_{1max} and ΔSUV_{max} were both strong predictors of pCR with excellent accuracies according to ROC tests (AUC= 0.89 and 0.90, respectively; 95%CI = 0.73-1.00 and 0.69-1.00, respectively; p<0.0001 for both). BF1 only tended to predict pCR (AUC=0.77; 95% CI =0.49-1.00; p=0.06) whereas SUV_{2max}, BF2, ΔBF and the SUV_{1max}/BF1 ratio did not. The ROC curve analysis combining ΔSUV and BF1 did not improved the AUC.

DISCUSSION

Functional imaging offers a unique opportunity to provide a non-invasive portrait of tumor biology. ¹⁸FDG-PET identifies patterns of tumor metabolism and blood flow depending on the biological characteristics of the breast cancer and the response to treatment.

Tumor Metabolism and Blood Flow at Baseline

The team from Seattle has also simultaneously quantify tumor BF and glucose metabolism using both ¹⁵O-water and dynamic ¹⁸FDG PET exams (15,23–26). Our baseline tumor BF values (BF1=0.21 vs 0.32 mL/min/g) and weak correlation between SUV1 and BF1 ($r= 0.22$ vs 0.39) parallel their results (25).

As in previous reports, a high baseline SUV correlated strongly with aggressive biological characteristics, including the TNBC tumor subtype (20,27). In contrast, and in accordance with the results of Dunnwald et al., we found no significant association between pre-therapeutic tumor BF and the tumor phenotypic features and subtypes (23). Tumor BF at baseline was only associated

with the patient's BMI, with higher tumor blood flow values in obese women. Previous studies have underlined the link between obesity and adipose tissue dysfunction with a pro-inflammatory and pro-angiogenic effect within the tumor micro-environment (28,29).

Specht et al. also demonstrated that an increased baseline tumor glucose metabolism to blood flow ratio was associated with the TNBC subtype (24). It was hypothesized that this ratio reflected hypoxia. Using dual ¹⁸FDG acquisitions, we also found that the baseline SUV/BF ratio was higher in women with TNBC subtype.

Monitoring the Response to Treatment and Prediction of pCR

After the first cycle of treatment, most tumors quickly exhibit significant decreases in both tumor metabolism and BF. But the correlation between these changes is rather weak. These two functional pathways may thus provide different and complementary biological information. Moreover, as for previous studies, huge differences in responses were observed across the breast cancer subtypes (7,20):

- HER2-positive tumors are highly chemo-sensitive to trastuzumab and show a drastic drop in both metabolism and BF after the first cycle of treatment. Contrary to the well-known high metabolic response, which is correlated with the final pathological response (9), the drastic drop in BF after the first cycle of Trastuzumab has never been reported. This is an interesting point because Trastuzumab has been demonstrated to have a strong anti-angiogenic effect (30).

- As previously demonstrated, good metabolic response in TNBC but lower metabolic response in Luminal/HER2-negative tumors was reported (20). The present

study reveals that the mean decrease in blood flow is low in both subtypes ($-22.5 \pm 51.2\%$ for TNBC tumors and $-2.7 \pm 70.6\%$ for luminal tumors) and varied considerably depending on the tumor, suggesting biological heterogeneity. The increase in BF observed in some tumors after the start of chemotherapy is an important issue. It may provide a valuable indication of tumor aggressiveness and chemo-resistance as adequate blood supply is crucial to sustain rapid growth and metastasis (31,32). In a recent alternative hypothesis, the increase in tumor BF in response to anti-angiogenic drugs or PI3K inhibitors was suggested to rather be a marker of treatment efficacy due to the transient “normalization” of the abnormal tumor vasculature (33).

The aim of monitoring the early tumor response during NAC is to predict final pCR and outcomes. Supporting our results, numerous studies have demonstrated that ^{18}F -FDG PET/CT accurately predicts the response to NAC in the HER2+ and TNBC subtypes (7,8). Kinetic parameters linked to vascular permeability and perfusion have also been investigated in this setting, using different imaging modalities:

- Sequential DCE-MRI: changes in the pharmacodynamic parameters, such as the AUC, the transfer constant (Ktrans) and the rate constant (kep) have been reported as early predictors of a tumor pCR to NAC (10–12,34)
- ^{15}O -water PET: a previous study found that the baseline tumor glucose metabolism to blood flow ratio correlated with the final pathological response, whereas baseline BF did not (25) : we found similar results using the dynamic ^{18}FDG first-pass model (Supl. Table 1). In other studies, women with persistent or elevated tumor BF on the interim PET experienced poorer tumor responses and outcomes (15,26).

Nonetheless, few studies have directly compared the blood flow and metabolic responses in the neoadjuvant setting of breast cancer (35). Tateishi et al performed FDG-PET/CT and DCE-MRI at baseline and after two cycles of NAC: PET/CT was more accurate than DCE MR in predicting a pCR (90.1% vs 83.8% for ΔSUV_{\max} and %kep, respectively), but no per-subtype analyses were performed (35).

The main originality of the present study is that in a single FDG PET exam, we combined a short PET dynamic first-pass model with the standard delayed PET acquisition, thus allowing a direct comparison of the early changes in ΔSUV_{\max} and in blood flow in their ability to predict the tumor histological response:

- Pooling all tumor subtypes together, ΔBF was the best perfusion parameter to predict pCR but showed poorer diagnostic accuracy on ROC analysis compared with the metabolic response assessed with ΔSUV_{\max} (AUC=0.65 vs 0.82, respectively)
- In a per-subtype analysis, the metabolic parameters systematically outperformed the perfusion parameters to predict pCR.

One limit of the study is that we did not determine its test-retest performance. PET biomarker predictive of responding/ non-responding tumors, may offer the opportunity to early tailor the NAC regimen for an individual patient. In HER2+ tumors, the AVATAxHER phase 2 randomized trial has assessed the benefit of adding bevacizumab in poorly-responding women after 2 cycles of trastuzumab/docetaxel ($\Delta\text{SUV} < 70\%$) (36). No PET-guided therapeutic strategy has been evaluated in the TNBC subtype. In women with TNBC, the addition of bevacizumab increases the pCR rate but is also associated with higher rates of toxicities (37). The role of anti-

angiogenic drugs in the neoadjuvant setting should be further evaluated but limited to biologically patient subsets most likely to benefit from this agent, such as women with no tumor blood flow response to conventional NAC regimen.

CONCLUSION

Baseline tumor glucose metabolism correlated with the biological markers of tumor aggressiveness, whereas tumor blood flow correlated with the patient's weight. Of these two biological hallmarks of cancer, the reduction in tumor metabolism was much more accurate to predict a pCR in the different subtypes of breast cancer. Randomized studies are needed to evaluate the clinical benefits of PET-based therapeutic strategies in the early stages of NAC in breast cancer.

DISCLOSURE: The authors have no conflicts of interest or financial disclosure to declare.

ACKNOWLEDGMENTS: We thank Mr Bastable for proof-reading the text.

REFERENCES

1. Mauri D, Pavlidis N, Ioannidis JPA. Neoadjuvant versus adjuvant systemic treatment in breast cancer: a meta-analysis. *J Natl Cancer Inst.* 2005;97:188-194.
2. Kuerer HM, Newman LA, Smith TL, et al. Clinical course of breast cancer patients with complete pathologic primary tumor and axillary lymph node response to doxorubicin-based neoadjuvant chemotherapy. *J Clin Oncol.* 1999;17:460-469.
3. von Minckwitz G, Untch M, Blohmer J-U, et al. Definition and impact of pathologic complete response on prognosis after neoadjuvant chemotherapy in various intrinsic breast cancer subtypes. *J Clin Oncol.* 2012;30:1796-1804.
4. Hanahan D, Weinberg RA. Hallmarks of cancer: the next generation. *Cell.* 2011;144:646-674.
5. Rousseau C, Devillers A, Sagan C, et al. Monitoring of early response to neoadjuvant chemotherapy in stage II and III breast cancer by [18F]fluorodeoxyglucose positron emission tomography. *J Clin Oncol.* 2006;24:5366-5372.
6. Avril S, Muzic RF, Plecha D, Traughber BJ, Vinayak S, Avril N. ¹⁸F-FDG PET/CT for Monitoring of treatment response in breast cancer. *J Nucl Med.* 2016;57(suppl 1):34S-9S.
7. Groheux D, Mankoff D, Espié M, Hindré E. ¹⁸F-FDG PET/CT in the early prediction of pathological response in aggressive subtypes of breast cancer: review of the literature and recommendations for use in clinical trials. *Eur J Nucl Med Mol Imaging.* 2016;43:983-993.
8. Humbert O, Riedinger J-M, Charon-Barra C, et al. Identification of Biomarkers Including 18FDG-PET/CT for early prediction of response to neoadjuvant chemotherapy in triple-negative breast cancer. *Clin Cancer Res.* 2015;21:5460-5468.
9. Humbert O, Cochet A, Riedinger J-M, et al. HER2-positive breast cancer: ¹⁸F-FDG PET for early prediction of response to trastuzumab plus taxane-based neoadjuvant chemotherapy. *Eur J Nucl Med Mol Imaging.* 2014;41:1525-1533.
10. Ah-See M-LW, Makris A, Taylor NJ, et al. Early changes in functional dynamic magnetic resonance imaging predict for pathologic response to neoadjuvant chemotherapy in primary breast cancer. *Clin Cancer Res.* 2008;14:6580-6589.
11. Johansen R, Jensen LR, Rydland J, et al. Predicting survival and early clinical response to primary chemotherapy for patients with locally advanced breast cancer using DCE-MRI. *J Magn Reson Imaging JMRI.* 2009;29:1300-1307.
12. Sun Y-S, He Y-J, Li J, et al. Predictive value of DCE-MRI for early evaluation of pathological complete response to neoadjuvant chemotherapy in resectable primary breast cancer: A single-center prospective study. *Breast Edinb Scotl.* 2016;30:80-86.
13. Tseng J, Dunnwald LK, Schubert EK, et al. 18F-FDG kinetics in locally advanced breast cancer: correlation with tumor blood flow and changes in response to neoadjuvant chemotherapy. *J Nucl Med.* 2004;45:1829-1837.

14. Zasadny KR, Tatsumi M, Wahl RL. FDG metabolism and uptake versus blood flow in women with untreated primary breast cancers. *Eur J Nucl Med Mol Imaging*. 2003;30:274-280.
15. Dunnwald LK, Gralow JR, Ellis GK, et al. Tumor metabolism and blood flow changes by positron emission tomography: relation to survival in patients treated with neoadjuvant chemotherapy for locally advanced breast cancer. *J Clin Oncol*. 2008;26:4449-4457.
16. Mullani NA, Herbst RS, O'Neil RG, Gould KL, Barron BJ, Abbruzzese JL. Tumor blood flow measured by PET dynamic imaging of first-pass 18F-FDG uptake: a comparison with 15O-labeled water-measured blood flow. *J Nucl Med*. 2008;49:517-523.
17. Cochet A, Pigeonnat S, Khoury B, et al. Evaluation of breast tumor blood flow with dynamic first-pass 18F-FDG PET/CT: comparison with angiogenesis markers and prognostic factors. *J Nucl Med*. 2012;53:512-520.
18. Humbert O, Berriolo-Riedinger A, Cochet A, et al. Prognostic relevance at 5 years of the early monitoring of neoadjuvant chemotherapy using (18)F-FDG PET in luminal HER2-negative breast cancer. *Eur J Nucl Med Mol Imaging*. 2014;41:416-427.
19. Humbert O, Riedinger J-M, Vrigneaud J-M, et al. 18F-FDG PET-Derived tumor blood flow changes after 1 cycle of neoadjuvant chemotherapy predicts outcome in triple-negative breast cancer. *J Nucl Med*. 2016;57:1707-1712.
20. Humbert O, Berriolo-Riedinger A, Riedinger JM, et al. Changes in 18F-FDG tumor metabolism after a first course of neoadjuvant chemotherapy in breast cancer: influence of tumor subtypes. *Ann Oncol*. 2012;23:2572-2577.
21. Mullani NA, Goldstein RA, Gould KL, et al. Myocardial perfusion with rubidium-82. I. Measurement of extraction fraction and flow with external detectors. *J Nucl Med*. 1983;24:898-906.
22. Neuhauser M. How to deal with multiple endpoints in clinical trials. *Fundam Clin Pharmacol*. 2006;20:515-523.
23. Dunnwald LK, Doot RK, Specht JM, et al. PET tumor metabolism in locally advanced breast cancer patients undergoing neoadjuvant chemotherapy: value of static versus kinetic measures of fluorodeoxyglucose uptake. *Clin Cancer Res*. 2011;17:2400-2409.
24. Specht JM, Kurland BF, Montgomery SK, et al. Tumor metabolism and blood flow as assessed by positron emission tomography varies by tumor subtype in locally advanced breast cancer. *Clin Cancer Res*. 2010;16:2803-2810.
25. Mankoff DA, Dunnwald LK, Gralow JR, et al. Blood flow and metabolism in locally advanced breast cancer: relationship to response to therapy. *J Nucl Med*. 2002;43:500-509.
26. Mankoff DA, Dunnwald LK, Gralow JR, et al. Changes in blood flow and metabolism in locally advanced breast cancer treated with neoadjuvant chemotherapy. *J Nucl Med*. 2003;44:1806-1814.
27. Gil-Rendo A, Martínez-Regueira F, Zornoza G, García-Veloso MJ, Beorlegui C, Rodriguez-Spiteri N. Association between [18F]fluorodeoxyglucose uptake and prognostic parameters in breast cancer. *Br J Surg*. 2009;96:166-170.

28. Mantovani A, Allavena P, Sica A, Balkwill F. Cancer-related inflammation. *Nature*. 2008;454:436-444.
29. Iyengar NM, Gucalp A, Dannenberg AJ, Hudis CA. Obesity and cancer mechanisms: tumor microenvironment and inflammation. *J Clin Oncol*. 2016;34:4270-4276.
30. Izumi Y, Xu L, di Tomaso E, Fukumura D, Jain RK. Tumour biology: herceptin acts as an anti-angiogenic cocktail. *Nature*. 2002;416:279-280.
31. Carmeliet P, Jain RK. Angiogenesis in cancer and other diseases. *Nature*. 2000;407:249-257.
32. Carmeliet P. Angiogenesis in life, disease and medicine. *Nature*. 2005;438:932-936.
33. Carmeliet P, Jain RK. Principles and mechanisms of vessel normalization for cancer and other angiogenic diseases. *Nat Rev Drug Discov*. 2011;10:417-427.
34. Choi WJ, Kim WK, Shin HJ, Cha JH, Chae EY, Kim HH. Evaluation of the tumor response after neoadjuvant chemotherapy in breast cancer patients: correlation between dynamic contrast-enhanced magnetic resonance imaging and pathologic tumor cellularity. *Clin Breast Cancer*. 2017 [Epub ahead of print].
35. Tateishi U, Miyake M, Nagaoka T, et al. Neoadjuvant chemotherapy in breast cancer: prediction of pathologic response with PET/CT and dynamic contrast-enhanced MR imaging--prospective assessment. *Radiology*. 2012;263:53-63.
36. Coudert B, Pierga J-Y, Mouret-Reynier M-A, et al. Use of [(18)F]-FDG PET to predict response to neoadjuvant trastuzumab and docetaxel in patients with HER2-positive breast cancer, and addition of bevacizumab to neoadjuvant trastuzumab and docetaxel in [(18)F]-FDG PET-predicted non-responders (AVATAHER): an open-label, randomised phase 2 trial. *Lancet Oncol*. 2014;15:1493-1502.
37. Sikov WM, Berry DA, Perou CM, et al. Impact of the addition of carboplatin and/or bevacizumab to neoadjuvant once-per-week paclitaxel followed by dose-dense doxorubicin and cyclophosphamide on pathologic complete response rates in stage II to III triple-negative breast cancer: CALGB 40603 (Alliance). *J Clin Oncol*. 2015;33:13-21.

FIGURE 1: Correlation between baseline tumor blood flow (BF), baseline glucose metabolism (SUV) and pCR

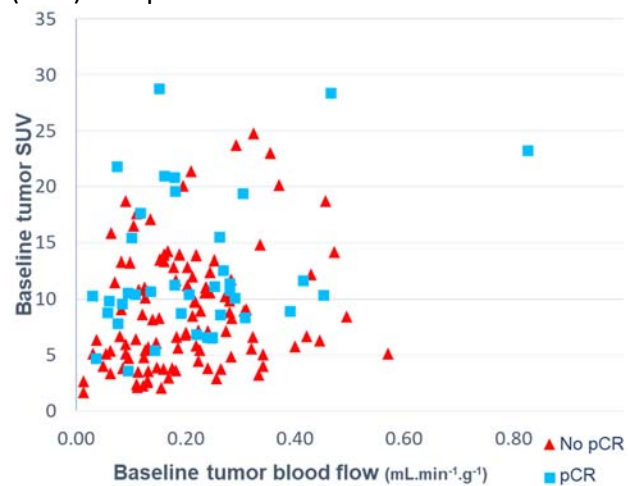


FIGURE 2 Correlation between tumor early blood flow changes (ΔBF), early glucose metabolism changes (ΔSUV) and pCR

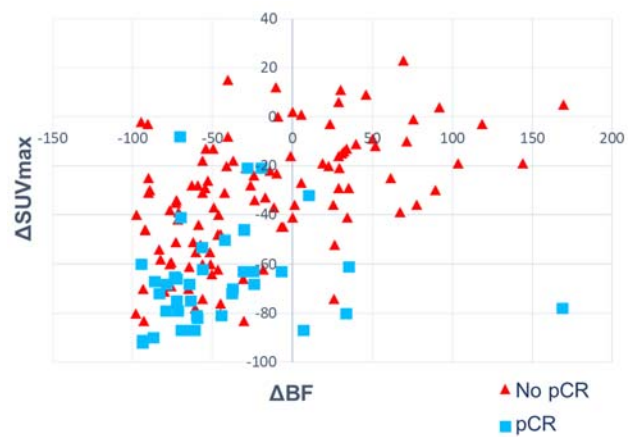


FIGURE 3 ROC curve analyses of best metabolic parameters for the prediction of pCR, considering tumor subtype

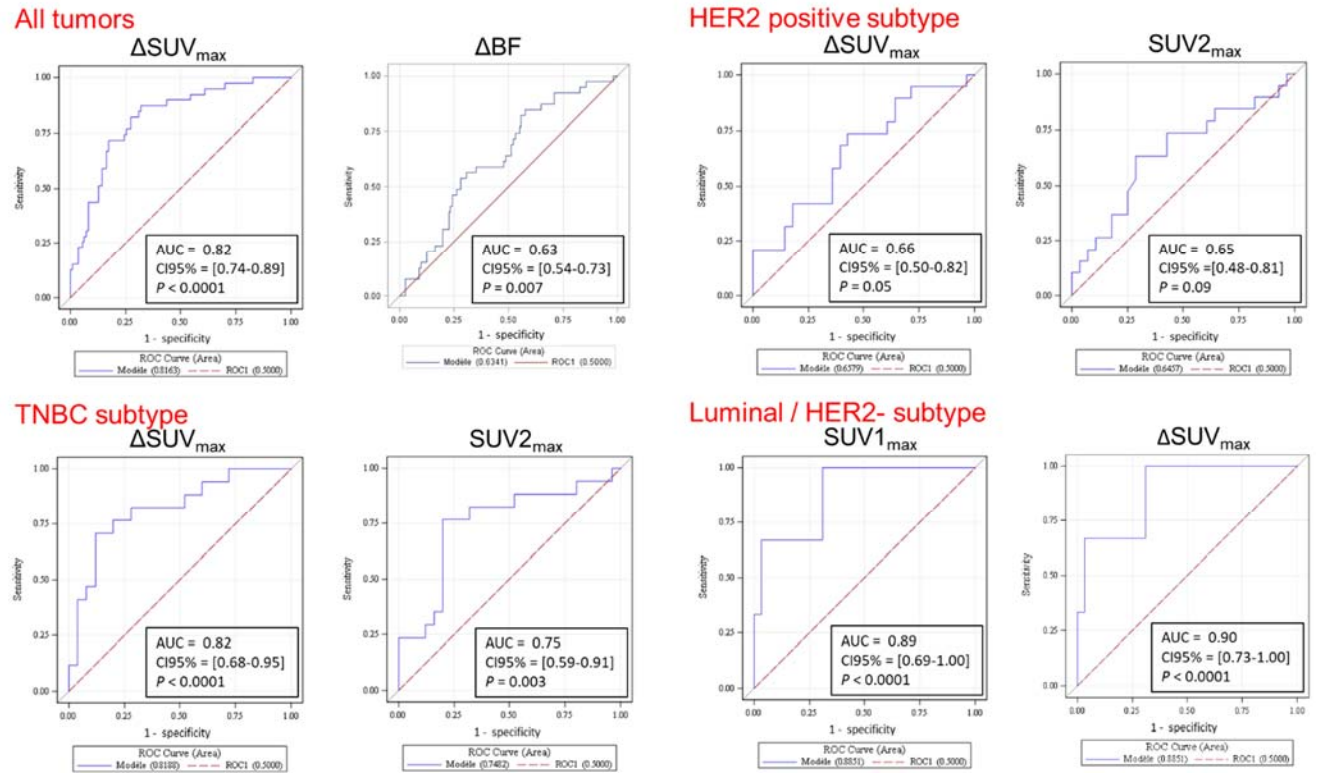


TABLE 1: Patients' characteristics

	N	%		N	%
Total patients	150	100	SBR – Number of mitosis		
			Score I	45	30
Age (years)			Score II	48	32
≤ 50	80	53.3	Score III	51	34
> 50	70	46.7	Unknown	6	4
BMI			Hormonal receptor status		
< 30	118	78.7	Negative	59	39.3
≥ 30	32	21.3	Positive	91	60.7
T Stage			Tumor phenotype		
T1-T2	128	85.3	HER 2	47	31.3
T3-T4	22	14.7	Luminal	61	40.7
Lymph node involvement			TNBC	42	28
No	58	38.7	Surgery		
Yes	92	61.3	Mastectomy	61	40.7
Histological type			Breast-conserving surgery	89	59.3
Ductal	139	92.7	pCR		
Lobular	9	6	ypT0/is		
Other	2	1.3	Yes	42	28.0
Tumor grading (SBR)			No	108	72.0
Grade I	7	4.7	ypN0		
Grade II	65	43.3	Yes	93	72.0
Grade III	75	50	No	57	38.0
Unknown	3	2	ypT0/is ypN0		
			Yes	39	26.0
			No	111	74.0

*pCR= pathological complete response

TABLE 2: Tumor metabolism and blood flow according to breast cancer subtype

	HER2 + (mean±SD)	TNBC (mean±SD)	Luminal/HER2 - (mean±SD)	P*
SUV_{1max}	9.5 ± 4.6	13. 9 ± 6.5	8.2 ± 5.2	<1.10⁻⁴
BF1 ml.min ⁻¹ .gr ¹	0.20 ± 0.11	0.22 ± 0.10	0.21 ± 0.15	NS [†]
SUV_{1max} / BF1	68.7 ± 66.3	79.2 ± 59.1	58.4 ± 52.5	0.011
ΔSUV (%)	-63.9 ± 20.1	-44.7 ± 27.1	-29.4 ± 23.0	<1.10⁻⁴
ΔBF (%)	-58.7 ± 30.2	-22.5 ± 51.2	-5.4 ± 59.6	1.10⁻⁴

Data are mean ± Standard Derivation (S.D).

*Kruskal-Wallis test

† NS = not significant.

Bold numerals correspond to statistically significant values, using the Bonferroni critical p value (multiple comparisons corrections), calculated at 0.01.

TABLE 3: Correlations between tumor PET imaging parameters and histo-biological characteristics of breast cancer

	SUV1_{max} P*	SUV2_{max} P*	ΔSUV P*	BF1 P*	BF2 P*	ΔBF P*
SBR grade (I-II vs III)	<0.001	0.002	0.040	NS [†]	NS	NS
BMI (cut-off = 30)	NS	0.023	NS	0.002	0.033	NS
Histological type (ductal vs lobular)	0.041	NS	NS	NS	NS	NS
HER2 over-expression (yes vs no)	NS	<0.001	<0.001	NS	<0.001	<0.001
HR[‡] status (Positive vs Negative)	<0.001	0.022	0.014	NS	NS	NS

*Mann–Whitney test.

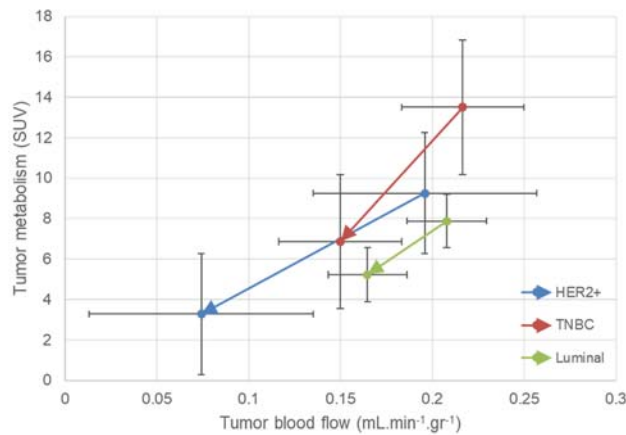
†NS = not significant.

‡HR = Hormonal receptors

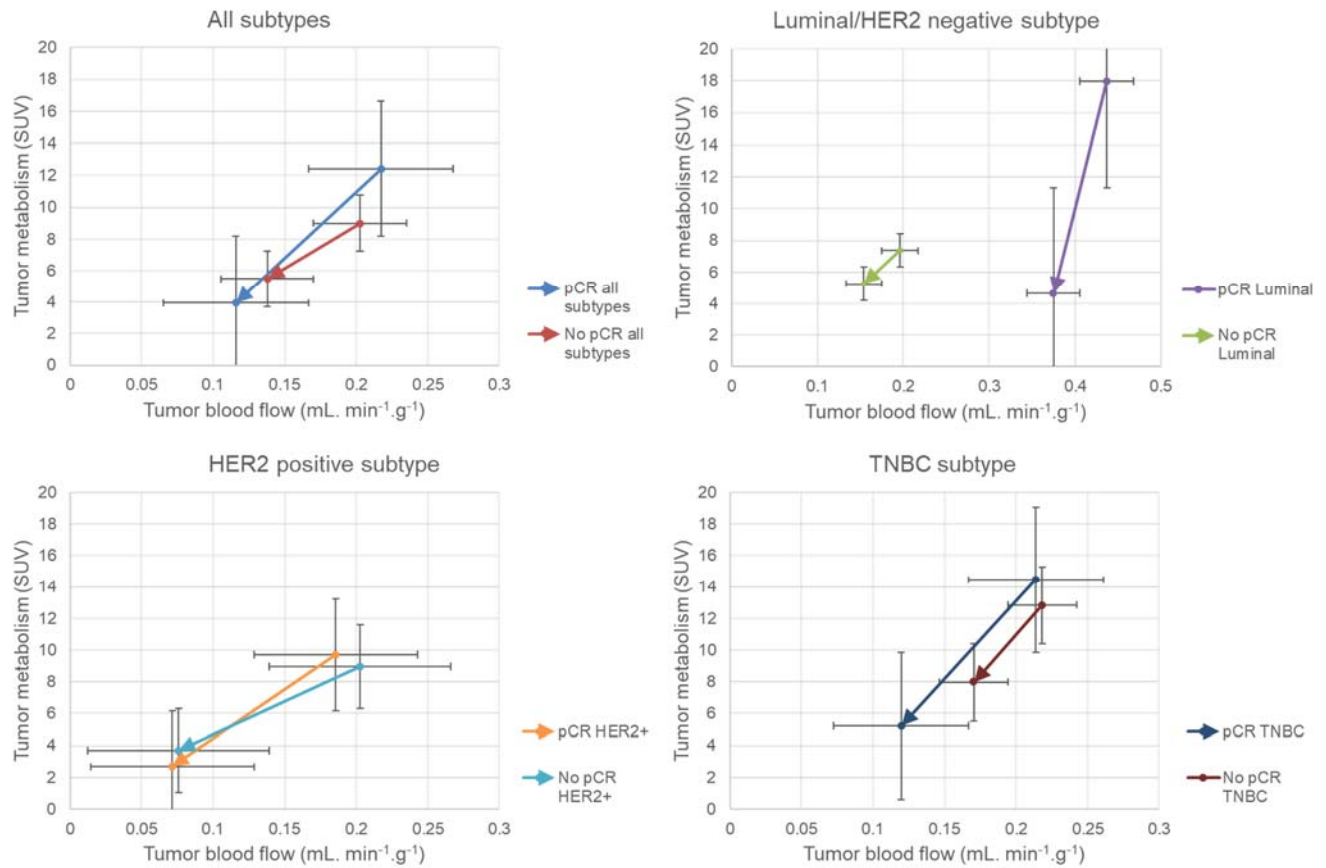
Bold numerals correspond to statistically significant correlations, using the Bonferroni critical p value (multiple comparisons corrections), calculated at 0.005.

Age, T stage, lymph node involvement and menopausal status were not significantly correlated with tumor imaging characteristics.

Supplemental FIGURE 1 Arrows show direction of changes in mean blood flow (BF) and mean glucose metabolism (SUV) of the 3 tumor subtypes, before and after the 1st cycle of neoadjuvant chemotherapy. Error bars represent standard error of mean.



Supplemental FIGURE 2 Arrows show direction of changes in mean blood flow (BF) and mean glucose metabolism (SUV), before and after the 1st cycle of neoadjuvant chemotherapy and considering final pathological response. Error bars represent standard error of mean.



SUPPLEMENTAL TABLE 1: ROC curves analyses for the prediction of pCR

	Area	CI 95%*	P
SUV1			
All tumors	0.67	0.58 - 0.77	0.0002
HER2 subtype	0.57	0.40 - 0.74	NS
TNBC subtype	0.58	0.41 - 0.76	NS
Luminal/HER2-	0.89	0.69 - 1.00	<10 ⁻⁴
SUV2			
All tumors			
HER2 subtype	0.65	0.48 - 0.81	NS
TNBC subtype	0.75	0.59 - 0.91	0.0027
Luminal/HER2-	0.50	0.03 - 0.98	NS
ΔSUV			
All tumors	0.82	0.74 - 0.89	<10 ⁻⁴
HER2 subtype	0.66	0.50 - 0.82	0.049
TNBC subtype	0.82	0.68 - 0.95	<10 ⁻⁴
Luminal/HER2-	0.90	0.73 - 1.00	<10 ⁻⁴
BF1			
All tumors	0.51	0.40 - 0.62	NS
HER2 subtype	0.55	0.37 - 0.74	NS
TNBC subtype	0.52	0.33 - 0.71	NS
Luminal/HER2-	0.77	0.49 - 1.00	NS
BF2			
All tumors	0.62	0.51 - 0.73	0.0269
HER2 subtype	0.56	0.38 - 0.74	NS
TNBC subtype	0.68	0.51 - 0.86	0.0399
Luminal/HER2-	0.67	0.19 - 1.00	NS
ΔBF			
All tumors	0.65	0.55 - 0.74	0.0031
HER2 subtype	0.53	0.35 - 0.70	NS
TNBC subtype	0.66	0.50 - 0.83	0.0554
Luminal/HER2-	0.41	0 - 0.97	NS
SUV1/BF1			
All tumors	0.62	0.51 - 0.72	0.0247
HER2 subtype	0.59	0.41 - 0.77	NS
TNBC subtype	0.58	0.39 - 0.77	NS
Luminal/HER2-	0.46	0.08 - 0.84	NS
ΔSUV and ΔBF combined			
All tumors	0.82	0.75 - 0.90	0.0001
HER2 subtype	0.72	0.57 - 0.88	0.0057
TNBC subtype	0.83	0.69 - 0.96	0.0001
Luminal/HER2-	0.68	0.52 - 0.84	0.0295

*Confidence Interval 95%

†NS = not significant.

Bold numerals correspond to statistically significant P values, using the Bonferroni critical value (multiple comparisons corrections), calculated at 0.0015.